ISBN: 978-3-95450-241-7 ISSN: 2673-5350 doi:10.18429/JACoW-IBIC2022-WEP15

XFEL PHOTON PULSE MEASUREMENT USING AN ALL-CARBON DIAMOND DETECTOR

C. Bloomer*,[1], L. Bobb, Diamond Light Source Ltd, Didcot, UK
M. E. Newton, University of Warwick, Coventry, UK
W. Freund, J. Grünert, J. Liu, European XFEL, Schenefeld, Germany
[1]also at University of Warwick, Coventry, UK

Abstract

The European XFEL can generate extremely intense, ultrashort X-ray pulses at MHz repetition rates. Single-crystal CVD diamond detectors have been used to transparently measure the photon beam position and pulse intensity. The diamond itself can withstand the power of the beam, but the surface electrodes can be damaged since a single pulse can already exceed the damage threshold of the electrode material. Presented in this work are pulse intensity and position measurements obtained at the European XFEL using a new type of all-carbon single-crystal diamond detector developed at Diamond Light Source. Instead of traditional surface metallisation, the detector uses laser-written graphitic electrodes buried within the bulk diamond. There is no metallisation in the XFEL X-ray beam path that could be damaged by the beam. The results obtained from a prototype detector are presented, capable of measuring the intensity and 1-dimensional X-ray beam position of individual XFEL pulses. These successful measurements demonstrate the feasibility of all-carbon diagnostic detectors for XFEL use.

INTRODUCTION

The European XFEL is a radiation source characterised by ultrashort pulse duration, high pulse intensities, high repetition rates, and almost complete transverse coherence. Individual pulses can contain up to 4 mJ of energy, delivered in a pulse that is less than 100 fs long [1,2]. It is important to monitor the XFEL pulse parameters such as intensity, beam size, and beam centroid position. Pulse-by-pulse capabilities are extremely useful as individual pulses vary considerably due to the stochastic nature of the light generation process in an XFEL. Making such measurements "transmissively", enabling the majority of the pulse energy to pass through the beamline into the instrument for the user experiment, is an increasingly important part of normalising data for fluctuations of the photon pulse parameters. Obtaining pulse-by-pulse X-ray beam size and position measurements in particular is extremely difficult, and there are very few techniques available that can achieve this. A general overview of XFEL beamline diagnostics can be found in Ref. [1].

On-line diagnostics that can be safely placed in the X-ray beam path and withstand the beam powers can be challenging to develop. Any beam instrumentation needs to be designed to survive the single-shot and multi-bunch beam intensities, while also making measurements of the X-ray beam without interfering with the beam delivery and user experiments. The peak power is sufficient to damage many materials placed in the beam path. Because of the extremely short pulse lengths, thermal transport does not remove any heat from intercepting diagnostics during the pulse duration itself, even for extremely good heat conductors such as copper or diamond [3], a factor exacerbated by the high repetition rate of the XFEL pulses in the MHz range. Under a sufficiently focused X-ray beam, most materials placed directly in the beam path will suffer ablation, and the upper layers of the material will vaporise due to absorption of energy from a single XFEL pulse. For this reason, instruments made of low atomic number materials such as diamond are useful, as photon absorption is lower resulting in lower absorbed power densities.

Single-crystal CVD diamond detectors show great promise for XFEL beam diagnostics. Compared to other detector materials, diamond has superior radiation tolerance, excellent thermal conductivity, and fast response times (i.e. fast charge carrier drift velocities). CVD diamond has found many uses at XFEL beamlines: as a scintillator screen material for beam profile imaging (when appropriately doped) [4], as a foil to generate backscattered photons for simple position or intensity monitoring [5], and most recently as solid-state ion-chamber flux intensity monitors [6,7]. The diamond itself can withstand the power of the beam, but the pulses can deposit sufficient energy into the detector that surface electrodes and other metallisation in the beam path may be damaged by the radiation.

Presented in this work are proof-of-principle pulse intensity and position measurements obtained at the European XFEL using a new type of all-carbon single-crystal diamond detector developed in collaboration between University of Warwick and Diamond Light Source.

DETECTOR DESIGN

The detector used for this work utilises laser-written graphitic electrodes, instead of traditional surface metallisation. These are fabricated using an ultrashort pulse laser technique. At the laser focal point there is sufficient energy deposited into the diamond that a local phase transition can take place: electrically non-conductive diamond is converted into conductive graphite. Diamond detectors using such electrodes were first demonstrated in the early 2010s [8].

These buried graphitic electrodes offer several advantages that make them more resistant to damage than surface metallised electrodes. Firstly, they very closely match the sur-

* chris.bloomer@diamond.ac.uk

ISBN: 978-3-95450-241-7 ISSN: 2673-5350 doi:10.18429/JACoW-IBIC2022-WEP15

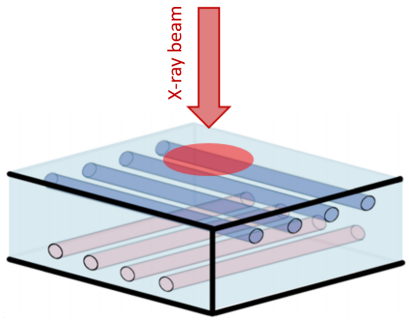

Figure 1: A sketch (not to scale) showing the electrode layout of the detector. The 'measurement' electrodes are shown in blue; the 'bias' electrodes are shown in red.

rounding diamond in terms of X-ray transmission, so the absorbed power density is much lower than that of typical titanium or aluminium electrodes, helping to prevent damage. Secondly, they are surrounded on all sides by thermally conductive diamond which can transfer away heat, unlike surface electrodes which are only connected to the diamond on one side. Finally, their thermal expansion better matches the diamond plate than surface metallisation, where a mismatch in the thermal expansion and contraction of the metallisation and the diamond can weaken the adhesion between the two and degrade the electrode.

The prototype detector used in this work has a series of buried 'strip electrodes' that can be individually read out to provide X-ray beam profile measurements. In brief, the diamond is a 'single crystal optical plus' grade CVD plate, 5.1 mm x 3.6 mm in size and 600 µm thick. The measurement strip-electrodes are located at a depth of 100 µm within the material, and the bias strip-electrodes are located at a depth of 200 µm. There is a spacing of 50 µm between each

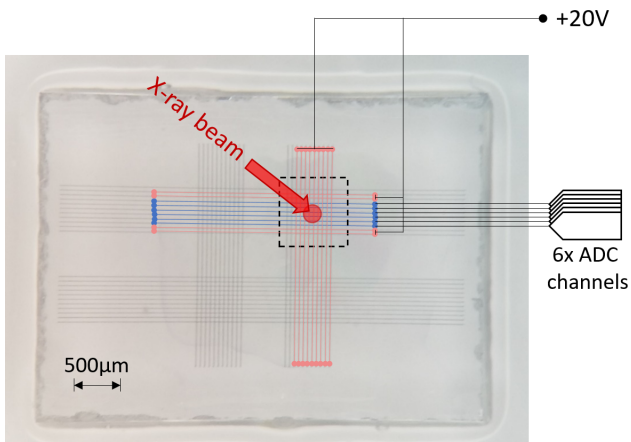

Figure 2: A photograph of the detector plate with the graphitic electrodes visible. The wiring arrangement is highlighted, showing how the 'bias' and 'measurement' electrodes are connected to the acquisition hardware. Biased 'guard rails' running parallel to the 'measurement' electrodes are used to ensure a uniform electric field within the interaction region.

individual strip-electrode. Figure 1 shows a sketch of this layout.

The graphitic electrodes are connected to the surface by vertical graphitic columns referred to as 'vias'. These are located at the edge of the diamond plate for the purpose of connecting the buried electrodes to a surface metallisation pad, well away from the centre of the detector where the beam would pass through. Further information on the design and operation of the detector, and beam profile measurements obtained from synchrotron radiation beamlines at Diamond Light Source, is presented elsewhere [9, 10]. Figure 2 shows a photograph of the diamond plate, illustrating how the strip electrodes were wired up to acquisition hardware used in these tests.

EXPERIMENTAL SET-UP

The Materials Imaging and Dynamics (MID) instrument [11] at European XFEL was used for these tests. The photon energy was 12.9 keV, and the average pulse energy before attenuation was 1.2 mJ. A CVD diamond filter was inserted upstream of the graphitic wire detector to attenuate the pulse energy for the duration of these proof-of-principle tests, and avoid damaging the detector, reducing the pulse energy at the graphitic wire detector to 0.17 mJ. The delivered beam contained 5 pulses per train at 10 Hz train repetition and 0.565 MHz intra-train pulse repetition rate (1770 ns gap between pulses in a train).

Compound refractive lenses were used to reduce the X-ray beam size at the detector to 250 µm. The diamond detector was installed at the instrument's sample point, at a distance of 970 m from the X-ray source point.

The MID instrument had six available fast ADC channels at the time of the tests, so these were connected to six of the parallel 'measurement' electrodes using lengths of coaxial cable. The ADCs were 16-bit commercial products with 108 MHz sampling rate, triggered to capture data synchronously with each pulse train.

The 'bias' electrodes were connected to a variable bias supply. For the duration of these experiments this was set to +20 V. The graphitic wires on either side of the parallel 'measurement' electrodes were also connected to the bias supply, to act as 'guard rails'. These guard rails provide two functions: to better constrain the electric field between 'measurement' and 'bias' electrodes, providing a more uniform field; and to restrict the fringe field found outside of the electrode array, and prevent extraneous charge carriers generated outside of the electrode array from being carried to the measurement electrodes.

Downstream of the location of the detector is the instrument's diagnostic end-station (DES). The DES includes tools for characterisation of the transmitted XFEL pulses, including a fast solid state intensity monitor capable of shot-by-shot measurements. This fast intensity monitor is also a diamond detector, without any position-sensing capabilities. The capabilities and operation of this intensity monitor is outlined in Ref. [6]. The intensity measurements from the graphitic

ISBN: 978-3-95450-241-7 ISSN: 2673-5350 doi:10.18429/JACoW-IBIC2022-WEP15

electrode detector can be compared to that from this existing DES intensity monitor.

BEAM INTENSITY MEASUREMENTS

The detector was installed on a motion stage to enable it to be scanned through the beam path. It was initially coarsely aligned using the stepper motor so that the X-ray beam was transmitted through the region indicated in Fig. 2. This enabled a measurement of the intensity of each of the pulses in the 5-pulse XFEL train. The ADC signal from one example train is presented in Fig. 3, along with the corresponding measurement from the DES intenstity monitor. It can be seen that there is agreement in the measured pulse heights.

Resolving the true pulse lengths (< 100 fs) is not possible for either instrument, but the pulse intensities can be compared. It is noted that a significant decay time is observed from the graphitic wire detector signals, compared to the MID intensity monitor. It is currently unclear if this is due to poor wiring or connection to the ADC, or due to some unwanted capacitances arising from within the detector. Future work should be carried out to address this question. Nonetheless, the individual pulses are clearly resolvable.

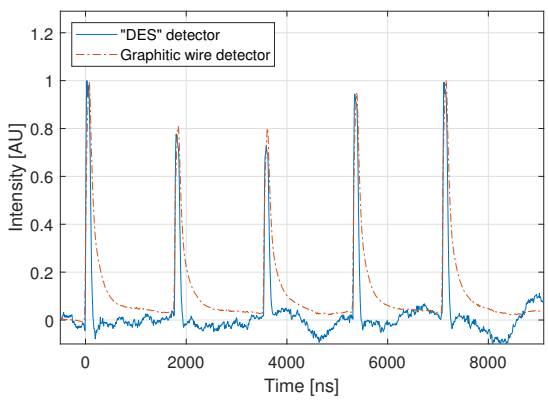

Figure 3: A measurement of the intensities of each pulse in the train. The measurement from the DES intensity monitor is compared with that from the graphitic wire detector. Intensities have been normalised to the peak intensity measured.

Figure 4 presents a comparison of measured pulse intensities from the graphitic wire detector and from the DES intensity monitor, observing the natural variation in pulse-by-pulse intensities during the experimental period. There is broad qualitative agreement between the two instruments, however the measured r.m.s. difference is 10.5 % of the graphitic wire intensity. This discrepancy is hypothesised to be due to the sensitive region of the graphitic wire detector being relatively small compared to the average incident beam size, so the full beam intensity is not measured if individual pulses vary significantly in size or position.

BEAM PROFILE MEASUREMENTS

By monitoring the signals recorded on all six acquisition channels individually, beam spatial profile information can

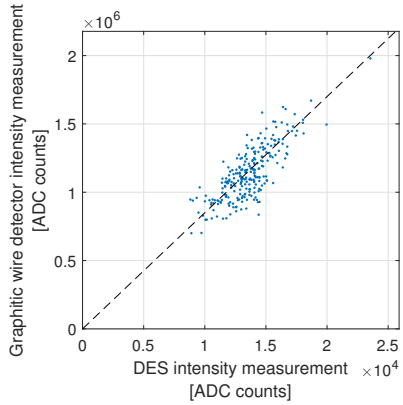

Figure 4: Pulse intensity measurements from the graphitic wire detector as a function of DES intensity measurement. A line of best fit is drawn.

be obtained. Shown in Fig. 5 is a the integrated measurement from the six channels over 20 pulse trains (100 pulses in total). Figure 6 shows the pulse profiles measured for a number of *individual* XFEL pulses from three trains.

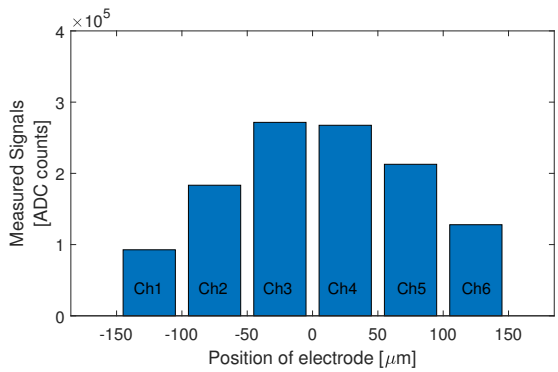

Figure 5: Vertical pulse profile measurements from the graphitic wire detector, showing the average profile obtained from 20 consecutive pulse trains.

BEAM POSITION MEASUREMENTS

A standard difference-over-sum (Δ/Σ) approach can be taken to obtain a measurement of the 1-dimensional X-ray beam position using this array of strip-electrodes.

$$Y_{\Delta/\Sigma} = \frac{(Ch1 + Ch2 + Ch3) - (Ch4 + Ch5 + Ch6)}{Ch1 + Ch2 + Ch3 + Ch4 + Ch5 + Ch6}$$

The motion stage that the detector was mounted upon was used to carry out a slow vertical stepper motor scan of the detector through the path of the XFEL beam whilst acquiring data from the six measurement electrodes. For each pulse during the scan the beam position was calculated, and is presented in Fig. 7. The dimensionless Δ/Σ is multiplied by an experimentally determined scale factor to convert it into a beam position with real-world units of millimetres. The calculated position of each individual XFEL pulse is

ISBN: 978-3-95450-241-7 ISSN: 2673-5350 doi:10.18429/JACoW-IBIC2022-WEP15

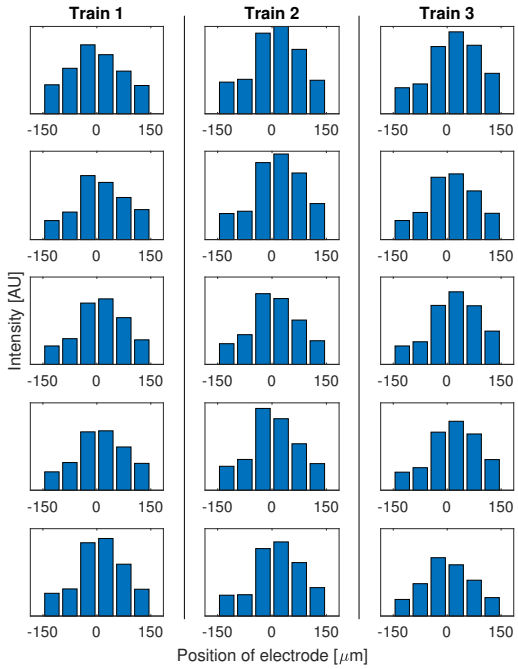

Figure 6: Vertical pulse profile measurements from individual pulses within three different 5-pulse trains.

shown in the figure (red dots), with the mean and standard deviation of the measured beam position at each step of the motor scan also displayed (blue error-bars).

The position measurement is found to be linear over about ± 0.3 mm, which is to be expected given the size of the incident beam and the electrode spacing. Stochastic shot-to-shot variation in beam position is clearly visible in this data. The measured standard deviation in individual pulse position was 0.043 mm.

FUTURE WORK

These experiments have demonstrated the feasibility of all-carbon profile monitors for XFEL pulse measurements, and indicated useful avenues for future research. This should be repeated with the full available pulse energy and maximum possible intra-train repetition rates, to demonstrate no adverse affect on the graphitic electrodes from the absorbed power. Repeating the measurements over a wider range of attenuations would also be useful to verify the intensity linearity of the detector.

The detector used in this test was optimised for 'continuous' synchrotron radiation, and not for 'RF' pulse-by-pulse measurements. Careful modelling could help produce a detector design that is better optimised for MHz XFEL measurements, and better capable of resolving individual pulses even at the highest repetition rates.

Finally, it would be beneficial to repeat these tests using new acquisition hardware with a greater number of ADC channels. This would allow for higher spatial resolution

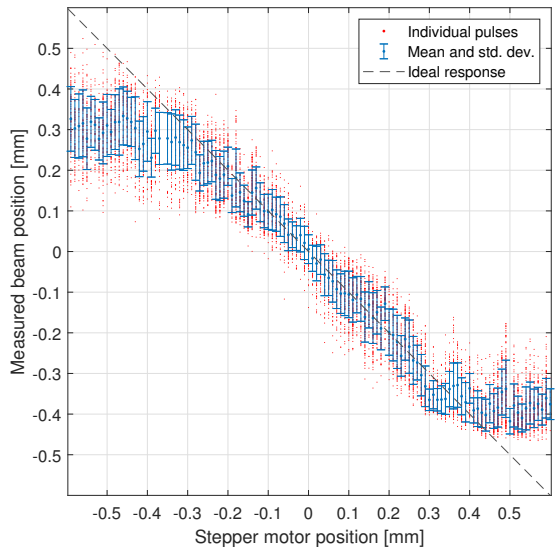

Figure 7: A scan of the detector motion stage, with a 1-dimensional beam position measurement acquired for each XFEL pulse during the scan.

than could be achieved using just the six channels that were available for these tests.

CONCLUSIONS

A proof-of-principle measurement of individual XFEL pulses arriving at MHz rates using an all-carbon graphitic electrode has been carried out. XFEL X-ray pulse intensity, 1-dimensional spatial profile, and position measurements have been obtained using the detector. The graphitic tracks survived exposure to the beam for the duration of the experiment and suffered no measurable damage.

ACKNOWLEDGEMENTS

The authors wish to acknowledge the support of many individuals and groups that aided in this research. The CVD diamond plate used to create this detector was provided by Element Six. We wish to acknowledge the contributions of P. Salter for the graphitic electrode fabrication, at the University of Oxford. The detector surface metallisation was carried out by B. Green, and the wire bonding by F. Courtney, both at the University of Warwick. Finally, the authors acknowledge the support and help of the MID instrument staff at European XFEL, in particular U. Boesenberg and A. Zozulya.

REFERENCES

[1] J. Grünert *et al.*, "X-ray photon diagnostics at the European XFEL", *J. Synchrotron Radiat.*, vol. 26, pp. 1422–1431, 2019. doi:10.1107/S1600577519006611

[2] W. Decking *et al.*, "A MHz-repetition-rate hard X-ray free-electron laser driven by a superconducting linear ac-

ISBN: 978-3-95450-241-7 ISSN: 2673-5350 doi:10.18429/JACoW-IBIC2022-WEP15

celerator", *Nat. Photonics*, vol. 14, pp. 391–397, 2020. doi:10.1038/s41566-020-0607-z

[3] T. Tschentscher *et al.*, "Photon Beam Transport and Scientific Instruments at the European XFEL", *Appl. Sci.*, vol. 7, p. 592, 2017. doi:10.3390/app7060592

[4] A. Koch *et al.*, "Design and initial characterisation of X-ray beam diagnostic imagers for the European XFEL", *Proc. SPIE Int. Soc. Opt. Eng.*, vol. 9512, p. 95121, 2015. doi:10.1117/12.2182463

[5] K. Tono *et al.*, "Single-shot beam-position monitor for x-ray free electron laser", *Rev. Sci. Instrum.*, vol. 82, p. 23108, 2011. doi:10.1063/1.3549133

[6] T. Roth *et al.*, "Pulse-resolved intensity measurements at a hard X-ray FEL using semi-transparent diamond detectors", *J. Synchrotron Radiat.*, vol. 25, p.p 177-188, 2017. doi:10.1107/S1600577517015016

[7] J. Bohon *et al.*, "Use of diamond sensors for a high-flux, high-rate X-ray pass-through diagnostic", *J. Synchrotron Radiat.*, vol. 29, pp. 595-601, 2022. doi:10.1107/S1600577522003022

[8] A. Oh *et al.*, "A novel detector with graphitic electrodes in CVD diamond", *Diamond Relat. Mater.*, vol. 38, pp. 9–13, 2013. doi:10.1016/j.diamond.2013.06.003

[9] C. Bloomer *et al.*, "A single-crystal diamond X-ray pixel detector with embedded graphitic electrodes", *J. Synchrotron Radiat.*, vol. 27, pp. 599–607, 2020. doi:10.1107/s160057752000140x

[10] C. Bloomer *et al.*, "Single-crystal diamond pixelated radiation detector with buried graphitic electrodes", in *Proc. IBIC'21*, Pohang, Korea, Sep. 2021, pp. 158-166. doi:10.18429/JACoW-IBIC2021-TUOA01

[11] A. Madsen *et al.*, "Materials Imaging and Dynamics (MID) instrument at the European X-ray Free-Electron Laser Facility", *J. Synchrotron Radiat.*, vol. 28, pp. 637–649, 2021. doi:10.1107/S1600577521001302